Study on IMC-PID Control for Single-phase Voltage-source UPS Inverters

Xu Yingnian[1], Zhao Yang[1,2], Kang Yong[1], Xiong Rui[1]
1. Department of Electrical Engineering, Huazhong University of Science and Technology, Wuhan, 430074,P.R.China
2. Department of Electrical Engineering, Hubei University of Technology, Wuhan, 430068,P.R.China

***Abstract*-A novel control scheme with PD output voltage instantaneous-value feedback inner loop for voltage-source inverter is proposed. The inner loop is designed to improve dynamic performance and the IMC-PID (internal model control-proportion integral derivation) external loop can ensure stable performance. The design methods of inner loop PD controller based on pole-assignment and external loop IMC-PID controller are discussed in detail. The control system is very simple and only the output voltage needs to be sampled. The PD inner controller and IMC-PID external controller are both easy to design and analyze. Simulation and experimental results are given to validate that the control scheme for voltage-source inverter proposed has not only nice dynamic and static performance but also strong robustness. The control scheme proposed has not only strong robustness, nice dynamic and static characteristics, but also easy to realization of the control algorithm in analog or digital.**

I. INTRODUCTION

Uninterruptible power supplies (UPS) are used to interface critical loads such as computers and communication systems to the utility system. The output voltage of the UPS inverter is required to be sinusoidal with minimum total harmonic distortion (THD) and invariant under large variation in loads[1]. Thus, many advanced techniques have been proposed, such as multiple feedback loop control[2], dead-beat control[3]-[4], repetitive control[5]-[7]，sliding mode control. The multiple feedback loop control is simple and easy to implement but this approach requires a comprehensive analysis on both open-loop and closed-loop frequency responses of the inverter control system for various controller parameters; The dead-beat control is sensitive to parameter variations and is complex to implement; The repetitive control can achieve low THD output in a few fundamental cycles, but its dynamic performance is not excellent; The sliding mode control has been proved quite useful against uncertainty. However, the well-known chattering problem must be especially taken care in analog or digital realization of the control algorithm [1].

In order to overcome the above disadvantages, the paper puts forward IMC−PID control scheme with the PD instantaneous-value feedback inner loop which is designed to improve dynamic performance while the IMC−PID external loop to ensure stable performance. The inner loop with a PD controller based on pole assignment technique not only improves the ability of the dynamic tracking and disturbance restraining, but also improves the robustness stability and static characteristics. The control scheme proposed has strong robustness，nice dynamic and static characteristics. Its control algorithm is also easy to realize in analog or digital control system.

The paper is organized as follow: Section II discusses the inter-model-control structure. How to select the nominal model of single-phase voltage-source inverter is presented in Section III. Section IV presents a design procedure for inner loop PD controller based on pole-assignment and external loop IMC-PID controller. The control block, static and dynamic performance and robustness performance of the proposed control scheme are presented in section V. A case design and its experimental results are presented in section VI. Finally, conclusions are drawn in section Ⅶ.

II. INTERNAL MODEL CONTROL

Fig.1 shows the IMC control system block diagram. P is the plant to be controlled, $\tilde{p}$ is the nominal model of plant, q is the controller and r , u , y are the reference, controller output and system output.

The IMC structure can be related to a classical feedback structure by the following equation,

$$c = \frac{q}{1 - q\tilde{p}} \tag{1}$$

where c is the classical feedback controller and the control structure is as shown in Fig. 2. The controller c has not only the simple structure of classical control but also IMC advantages such as excellent tracking performance, attenuation disturbance ability and strong robustness with little modeling effort[8]-[9].

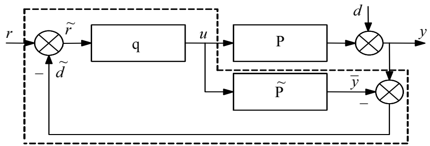

Fig. 1 Block diagram of IMC system

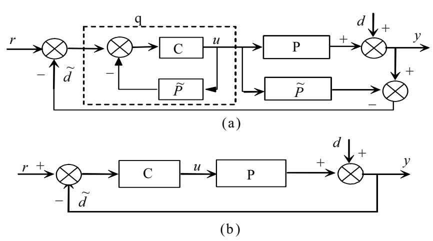

Fig. 2 Diagram of relationship between IMC and classical control system

978-1-4244-1718-6/08/$25.00 ©2008 IEEE

Authorized licensed use limited to: ELETTRONICA E INFORMATICA PADOVA. Downloaded on June 7, 2009 at 06:08 from IEEE Xplore. Restrictions apply.

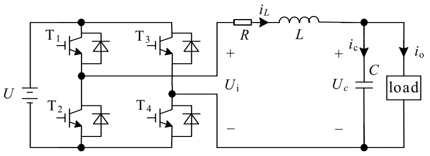

Fig. 3 Single phase voltage-resource inverter power circuit

III. Inverter Model

A single phase full-bridge inverter is shown in Fig.3. The symbol U represents the DC voltage source, u_i is the inverter bridge output voltage; u_c is the voltage of filter capacitance C, i_L is the current of filter inductance L and i_o is the load current; R is the equivalent damping resistance.

The differential equation model can be derived by applying KVL and KCL as follow:

$$\frac{\mathrm{d}u_c}{\mathrm{d}t} = \frac{1}{C} i_L - \frac{1}{C} i_o \tag{2}$$

$$\frac{\mathrm{d}i_L}{\mathrm{d}t} = \frac{1}{L} u_i - \frac{1}{L} u_c - \frac{R}{L} i_L \tag{3}$$

The inverter transfer function with no load can be derived from equation (2) and (3) as follow:

$$G_0(s) = \frac{U_C(s)}{U_i(s)} = \frac{\omega_n^2}{s^2 + 2\xi\omega_n s + \omega_n^2} = \frac{1}{LCs^2 + RCs + 1} \tag{4}$$

where ω_n is the undamped natural frequency, $\omega_n = \sqrt{1/LC}$; ξ is the damping ratio, $\xi = R/2\sqrt{C/L}$.

In order to simplify the multiplicative uncertainty function, the paper chooses the mathematical model $G_0(s)$ at no load as the inverter nominal model and regards the load current as disturbance. The multiplicative uncertainty function $l_m(s)$ is:

$$l_m(s) = \frac{(LC - L'C')s^2 + (RC - R'C')s}{L'C's^2 + R'C's + 1} \tag{5}$$

where L', C', R' are practical inductance, capacitance and damped resistance, respectively.

IV. IMC-PID Controller Design

A Inner Loop Controller Design

From Fig.1, the relationship as follow can be derived:

$$Y(s) = \frac{P(s)Q(s) \cdot R(s)}{1 + Q(s)[P(s) - \tilde{P}(s)]} + \frac{\left[1 - \tilde{P}(s)Q(s)\right] \cdot D(s)}{1 + Q(s)[P(s) - \tilde{P}(s)]} \tag{6}$$

Assuming that the nominal model is accurate, $\tilde{P}(s) = P(s)$, then the follow equation can be gotten.

$$Y(s) = P(s)Q(s)R(s) + (1 - P(s)Q(s))D(s) \tag{7}$$

Equation (7) shows that the response of system input $R(s)$ and the attenuation of system disturbance $D(s)$ all have the relation with the plant pole. The damping ratio ξ of $G_0(s)$ is so small that the inverter has bad dynamic performance and the THD of inverter output voltage with nonlinear load is high. However, the IMC hasn't the ability to improve it in this case [9]. To overcome the shortcoming of IMC, the paper puts forward IMC-PID control scheme with the PD instantaneous-value feedback inner loop. The PD inner loop is designed to improve the inverter dynamic performance.

The inner PD controller is designed based on pole assignment[5]. Selecting capacitor voltage u_c and capacitor current i_c as state variables, and inverter bridge output voltage u_i as the input, the state different equation at no load is:

$$\begin{bmatrix} \dot{u}_c \\ \dot{i}_c \end{bmatrix} = \begin{bmatrix} 0 & 1/C \\ -1/L & -R/L \end{bmatrix} \begin{bmatrix} u_c \\ i_c \end{bmatrix} + \begin{bmatrix} 0 \\ 1/L \end{bmatrix} u_i \tag{8}$$

$$\boldsymbol{y} = \begin{bmatrix} 1 & 0 \end{bmatrix} \begin{bmatrix} u_c \\ i_c \end{bmatrix} \tag{9}$$

By adding state feedback: $k\boldsymbol{x} = (k_1 u_c + k_2 i_c)$, we can get the expect close-loop poles as follow.

$$p_{1,2} = -\xi_1\omega_1 \pm j\sqrt{(1-\xi_1^2)}\omega_1 \tag{10}$$

where ξ_1 is the expect damped ratio, ω_1 is the expect undamped natural frequency. State feedback gain k_1 , k_2 are as follow:

$$k_1 = \omega_1^2 LC - 1 , \quad k_2 = 2\xi_1\omega_1 L - R$$

The product of C and du_c/dt is i_c , so the capacitor current feedback i_c can be changed to capacitor voltage differential feedback du_c/dt . Thus, the equipment of voltage test doesn't be needed and the cost of inverter is reduced. From above analysis, the parameters of inner PD loop can be gotten as follow.

$$\begin{cases} K_P = k_1 = \omega_1^2 LC - 1 \\ K_D = k_2 \cdot C = 2\xi_1\omega_1 LC - RC \end{cases} \tag{11}$$

B External Loop IMC-PID Controller design

There are many methods to design the IMC controller. The widely used method is as follow.

Step1 Factor the nominal model $\tilde{P}(s)$.

The nominal model $\tilde{P}(s)$ is decomposed as follow.

$$\tilde{P}(s) = \tilde{P}_+(s)\tilde{P}_-(s)$$

where $\tilde{P}_+(s)$ contains all the time delays and the parts whose poles in the right complex plane of $\tilde{P}(s)$; $\tilde{P}_-(s)$ is stable and does not involve predictors. The nominal model of inverter with the inner PD loop is as follow.

Authorized licensed use limited to: ELETTRONICA E INFORMATICA PADOVA. Downloaded on June 7, 2009 at 06:08 from IEEE Xplore. Restrictions apply.

$$\tilde{p}(s) = \frac{\omega_n^2}{s^2 + (2\xi\omega_n + K_D\omega_n^2)s + (1+K_P)\omega_n^2} \tag{12}$$

where $\tilde{P}_-(s) = \omega_n^2 / [s^2 + (2\xi\omega_n + K_D\omega_n^2)s + (1+K_P)\omega_n^2]$, $\tilde{P}_+(s) = 1$.

Step2 Get the IMC controller and classical controller

Define the IMC controller $Q(s)$ by

$$\begin{aligned} Q(s) &= \tilde{P}_-^{-1}(s)F(s) \\ &= F(s)[s^2 + (2\xi\omega_n + K_D\omega_n^2)s + \omega_n^2]/\omega_n^2 \end{aligned}$$

where $F(s)$ is the first order filter, $F(s) = 1/(\tau s + 1)$. According to equation (1), the classical controller can be derived as follow.

$$C(s) = \frac{s^2 + (2\xi\omega_n + K_D\omega_n^2)s + (1+K_P)\omega_n^2}{\tau\omega_n^2 s} \tag{13}$$

Step3 Change the classical controller to traditional PID controller.

The PID controller structure is assumed as follow.

$$G_{pid} = k_p + k_i\frac{1}{s} + k_d s = \frac{k_d s^2 + k_p s + k_i}{s} \tag{14}$$

From equation (13) and (14), we can get:

$k_p = (2\xi\omega_n + K_D\omega_n^2)/\tau\omega_n^2$, $k_i = (1+K_P)/\tau$, $k_d = 1/\tau\omega_n^2$, where τ is the filter coefficient.

The inverter nominal model with inner PD loop is shown in equation (12). The multiplicative uncertainty function $l_m(s)$ is:

$$l_m(s) = \frac{(LC - L'C')s^2 + (RC - R'C')s}{L'C's^2 + (R'C' + K_D)s + 1 + K_P} \tag{15}$$

In order that the control system has robust stability, the following equation must be satisfied.

$$\left|\eta(\mathrm{j}\omega)\tilde{l}_m(\omega)\right| \le 1$$

where $\eta(\mathrm{j}\omega)$ is the complementary sensitivity function; $\tilde{l}_m(\omega)$ is the bound of multiplicative uncertainty function. This paper first gets the $\tilde{l}_m(\omega)$ in the case of $0.5L \le L' \le 1.5L$, $0.5C \le C' \le 1.5C$, $0.5R \le R' \le 1.5R$, then confirms the filter constant τ by $\eta(\mathrm{j}\omega)$. The smaller τ is, the better dynamic and static performance the system has. On the other hand, the bigger τ is, the stronger robustness the system has. Thus, in principle, the filter coefficient τ should be determined such that an optimal compromise between the performance and robustness is reached[8]-[9].

V. SYSTEM PERFORMANCE ANALYSIS

A Block Diagram of Control System

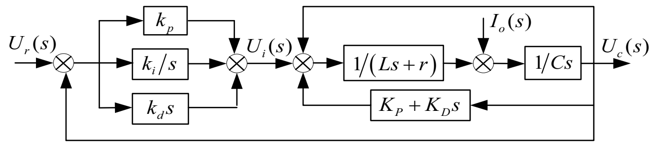

Fig.4. Block diagram of Inverter IMC-PID control system with PD instantaneous-value feedback inner loop

Fig. 4 shows the block diagram of the inverter control system based on IMC-PID control scheme with the PD instantaneous-value feedback inner loop.

In Fig.4, U_r is the sinusoidal input reference. According to block diagram above, the closed-loop transfer function of output voltage U_c and the sinusoidal input reference U_r and the load current disturbance signal I_o is shown as

$$\begin{aligned} U_c(s) &= \frac{\left(k_d s^2 + k_p s + k_i\right)\cdot U_r(s)}{LCs^3 + (RC + K_D + k_d)s^2 + (1 + K_P + k_p)s + k_i} \\ &\quad - \frac{(Ls+R)s \cdot I_o(s)}{LCs^3 + (RC + K_D + k_d)s^2 + (1 + K_P + k_p)s + k_i} \\ &= \frac{1}{1+\tau s}U_r(s) - \frac{s/C + R/LC}{s^2 + 2\xi_1\omega_1 s + \omega_1^2}\cdot\frac{\tau s}{1+\tau s}I_o(s) \end{aligned} \tag{16}$$

B Dynamic Characteristics

The system response of suddenly switching on or switching off load shows the inverter dynamic characteristics. From equation (16), the closed-loop transfer function of output voltage U_c with the load current I_o is shown as

$$\frac{U_c(s)}{I_o(s)} = \frac{(Ls + r)}{LCs^2 + (rC + K_D)s + 1 + K_P}\cdot\frac{\tau s}{1+\tau s} \tag{17}$$

The system load response performance is mainly determined by the poles of the transfer function in equation (17). τ is much small, so the transfer function is equivalent to a second-order system. The dynamic characteristic can be satisfied with expected ξ_1, ω_1.

C Static Characteristics

The frequency response of closed-loop output voltage U_c can be derived by equation (16) with $s = j\omega$. The static value of U_c is composed of two parts: one part caused by input voltage U_r and the other part caused by load current disturbance I_o. The former one is regarded as the output voltage of the closed-loop system at no load, while the latter one as the voltage drop on the system inner impedance. Without considering the harmonic current, the output voltage U_c can be shown as

$$U_c(j\omega) = U_{or}(j\omega) + U_{oj-b}(j\omega) \tag{18}$$

The output U_{or} caused by U_r and the voltage drop U_{oj-b} caused by fundamental load current can be derived from equation (16).

Authorized licensed use limited to: ELETTRONICA E INFORMATICA PADOVA. Downloaded on June 7, 2009 at 06:08 from IEEE Xplore. Restrictions apply.

D Robustness Performance Analyze

The model uncertainty caused by parameter uncertainty is called structure uncertainty, which is the main reason of inverter model uncertainty at no load. The inverter nominal model structure uncertainty is mainly caused by change of damping resistance *R*, output filter inductance *L* and output filter capacitance *C*. It exist error in parameter *L*, *C* and *R* because of the difficulty of measuring the damping resistance and deviation of inductance and capacitance rating value. The closed-loop frequency characteristic indicates the tracking performance, and the disturbance frequency characteristic indicates the ability to attenuate disturbance. So, the control system robustness performance can be analyzed by its closed-loop frequency characteristic and disturbance frequency characteristic. The closed-loop transfer function $G_r(s)$ and load disturbance transfer function $G_{I_o}(s)$ can be derived from equation (16)

$$G_r(s) = \frac{k_d s^2 + k_p s + k_i}{LCs^3 + (rC + K_D + k_d)s^2 + (1 + K_P + k_p)s + k_i}$$

$$G_{I_o}(s) = \frac{U_c(s)}{-I_o(s)} = \frac{Ls + r}{LCs^2 + (rC + K_D)s + 1 + K_P} \frac{\tau s}{1 + \tau s}$$

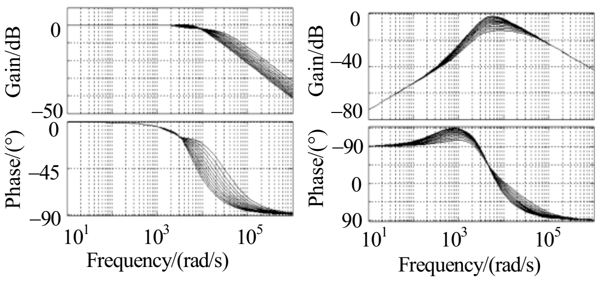

(a) (b)

Fig.5. Frequency characteristic when *L* changes between ±50%

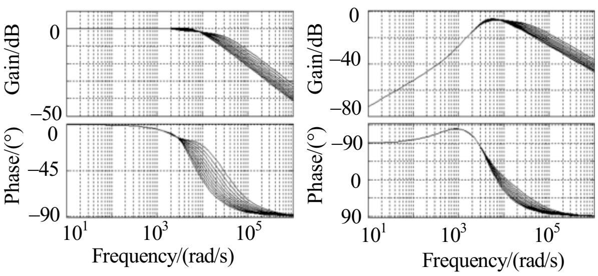

(a) (b)

Fig.6. Frequency characteristic when *C* changes between ±50%

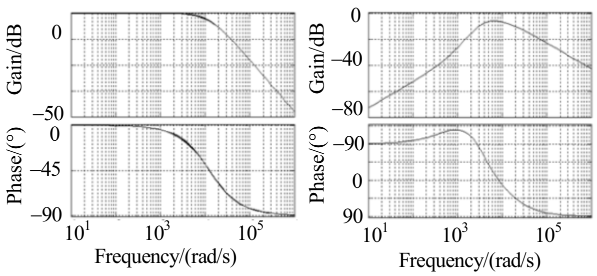

(a) (b)

Fig.7. Frequency characteristic when *R* changes between ±50%

Fig. 5 shows closed-loop transfer function bode diagram and disturbance transfer function bode diagram when the parameter *L* varies at ±50% . Fig.5(a) shows that the closed-loop frequency characteristic has no change at the low frequency band, a little difference at the medium frequency band, and the gain at the high frequency band ranges from -3.5dB to 4.78dB. Fig.5(b) shows that the change of *L* only affects the medium frequency band gain which ranges from -3.52dB to 6.78dB, and there is no change at the low and high frequency band.

Fig.6 shows the closed-loop transfer function bode diagram and disturbance transfer function bode diagram when the parameter *C* varies at ±50% . Fig.6(b) shows that the change of *C* only affects the high frequency band gain which ranges from -3.3dB to 4.9dB.

Fig.7 shows the closed-loop transfer function bode diagram and disturbance transfer function bode diagram when the parameter *R* varies at ±50% . It shows that the change of *R* hardly affects the system performance.

The above simulation results show that the change of parameter *L*, *C*, *R* have little influence on the system response performance, which means that the closed-loop system has strong robustness. And it can regard the resistance of the output filter inductor as the damping resistance in practice because the error of parameter *R* hardly affects the system performance.

VI. Simulation and Experimental Results

A Power Circuit Parameter

Fig.3. shows the inverter power circuit which adopts single phase full bridge circuit. Its characteristics are indicated in Table I. The nonlinear load adopts the diode bridge rectifier with a *LC* output filter and a resistance. In order to design the controller, the expect damping ratio ξ is 0.707, the undamped natural frequency ω_n is 3700rad/s, and the filter coefficient τ is 8e-5. The controller parameters are designed as $K_P = 0.058$, $K_D = 3.6231 \times 10^{-4}$, $k_p = 5.0571$, $k_i = 1.3225 \times 10^4$, $k_d = 9.6612 \times 10^{-4}$.

B Simulation and Experimental Results

Fig. 8(a) and (b) show the simulated and experimental output voltage and current waveforms, respectively. In Fig. 8(a), the results are achieved at the rating resistance load. In Fig. 8(b), the results are achieved at 85% of rating resistance load. Output voltage THD in simulation and experiment are both less than 1%.

Fig. 9(a) shows the simulated output voltage and current waveforms at suddenly switching on or switching off 70% rating resistance load. Fig.9(b) shows the experimental output voltage and current waveforms at suddenly switching on 70% rating resistance load. The dynamic processes of simulation or experiment are less than 1.5ms. And the output voltage changes are less than 7%.

Authorized licensed use limited to: ELETTRONICA E INFORMATICA PADOVA. Downloaded on June 7, 2009 at 06:08 from IEEE Xplore. Restrictions apply.

TABLE I.
Power Circuit CHARACTERISTICS

Main Circuit Characteristic	Value
IGBT	1200V/100A
output filter inductance (mH)	0.552
equivalent resistance (Ω)	0.3
output filter capacitance (μF)	140
switch frequency (kHz)	7.2
rating output voltage (V)	110
rating output resistant current (A)	20
rating power factor	0.7

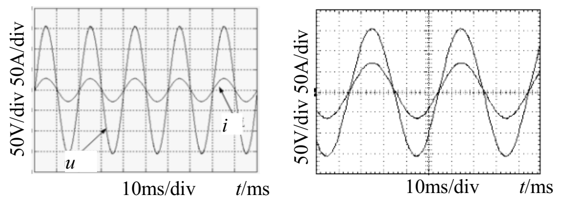

(a) (b)

Fig. 8. Inverter output voltage and current waveforms with resistance load

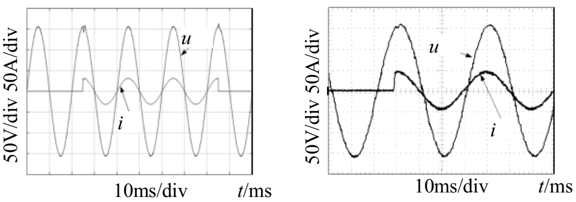

(a) (b)

Fig. 9. Inverter output voltage and current waveforms with resistance load

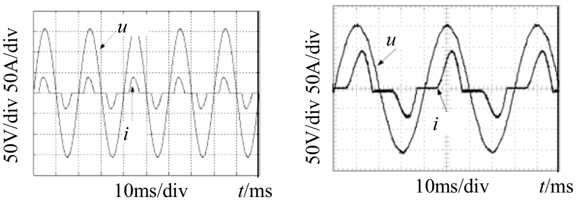

(a) (b)

Fig. 10. Inverter output voltage and current waveforms with nonlinear load

Fig. 10(a) and (b) show the simulated and experimental output voltage and current waveforms at nonlinear load when the load current peak value is 38A, respectively. Output voltage THD in simulation and experiment are 0.36% and 1.59%, respectively.

The simulation and experiment results both show that the proposed control system has good dynamic performance, high static precision and is suitable for various load conditions especially nonlinear load condition because of its strong ability to restrain the waveform distortion.

VII. CONLUSION

This paper proposes the inverter IMC-PID control system with the PD instantaneous-value feedback inner loop for the first time. The control system is easy to design, analyze and implement, which only needs the output voltage to be sampled. The simulation and experimental results show that the proposed control system has good dynamic and static performance and strong robustness. It has no need to measure the damping resistance because the error of damping resistance has no effect on system performance. Compared with the other control scheme, the proposed inverter control scheme has simpler structure, lower cost and stronger robustness. So, the IMC-PID inverter control system with PD instantaneous-value feedback inner loop is a good inverter control scheme with practicable value.

REFERENCES

[1] Tzann-Shin Lee, S. J. Chiang, and Jhy-Ming Chang, “Loop-shaping controller designs for the single-phase UPS inverters,” *IEEE Trans. Power Electon.*, vol. 16, no.4, pp. 473-481, 2001

[2] Abdel-Rahim M, and Quaicoe J E, “Analysis and design of a multiple feedback loop control strategy for single-phase voltage-source UPS inverter,” *IEEE Trans. Power Electronics*, vol. 11, no.4, pp. 532-541, 1996

[3] Kukrer O, “Deadbeat control of three-phase inverter with an output LC filter,” *IEEE Trans. Power Electronics*, vol. 11, no.1, pp. 16-23, 1996

[4] Hua C. “Two-level switching pattern deadbeat DSP controlled PWM Inverter,” *IEEE Trans. Power Electronics*, vol. 10, no.5, pp. 310-317, 1995

[5] Zhang kai,, *Study on Repetitive Control Theory Based Waveform Correction Technique for CVCF-PWM Inverters*, Doctor dissertation. Wuhan: Huazhong University of Science and Technology, 2000

[6] Li Jian, Kang Yong, and Chen Jian, “A hybrid fuzzy-repetitive control scheme for 400HZ CVCF inverter,” *Proc. CSEE*, vol. 25, no.9, pp. 54-61, 2005

[7] Zhang Kai, Peng Li, and Xiong Jian, ”State-feedback-with-integral control plus repetitive control for PWM Inverters,” *Proc. CSEE*, vol. 26, no.10, pp. 56-62, 2006

[8] Lü Zhaoxia, *Rearch on Internal Model Control for Nonlinear System*, Doctor Dissertation, Nanjing: Nanjing University of Science and Technology, 2000

[9] Xu Yingnian, *Research on Waveform Control Technique For SPWM Inverters Based on IMC-PID*, Master Dissertation, Wuhan: Hua-zhong University of Science and Technology，2005

Authorized licensed use limited to: ELETTRONICA E INFORMATICA PADOVA. Downloaded on June 7, 2009 at 06:08 from IEEE Xplore. Restrictions apply.